Journal of Civil Engineering and Urban Planning (2025)
Clausius Scientific Press, Canada

DOI: 10.23977/jceup.2025.070108
ISSN 2616-3969 Vol. 7 Num. 1

Numerical analysis and force transfer mechanism of PBL connector in steel-UHPC structure

Sen Xiong

College of Civil Engineering, Southwest Forestry University, Kunming, 650000, China

Keywords: Combined Structure; UHPC; PBL Connector; Finite Element Analysis; Force Transfer Mechanism

Abstract: Finite element analysis is used to study the numerical analysis and force transfer mechanism of PBL connectors in steel-UHPC structure. Based on the calculated test results, the finite element model is built, the whole process of connector force is analyzed and the parameters are analyzed. After the test verification, the load-slip curve and the test curve are relatively high, and the peak load ratio is between 0.96 and 0.98, with an error of <10%, which can accurately predict the bearing capacity and stress state of the PBL connector. Force transmission mechanism: in the elastic stage, the shear force is shared by the concrete tenon and the steel bar, and the concrete proportion is high; in the elastic-plastic stage, the concrete tenon is gradually plastic, and the load proportion of the steel bar increases; during the limit damage, the concrete tenon damage is obvious, and the steel bar yields, and the test piece loses the bearing capacity. The shear resistance of penetrating reinforcement and concrete tenon are the key to determine the shear bearing capacity of PBL connector. Reasonable selection of UHPC compressive strength, opening steel plate thickness, through the reinforcement yield strength and opening diameter, can effectively improve the mechanical properties of PBL connector. This study provides theoretical support for the design and optimization of PBL connector in the steel-UHPC combination structure.

1. Introduction

1.1 Research Background and Significance

At present, the research on PBL connector mainly focuses on traditional concrete materials, while the research on PBL connector in UHPC is relatively few. Although some experimental studies have explored the stress performance of PBL connector in UHPC, it is difficult to fully reveal the microscopic force state and force transfer mechanism due to the limitation of test conditions. Therefore, with the help of numerical simulation method, especially finite element analysis, can make up for the deficiency of experimental research, explore the whole process of PBL connector in UHPC, reveal the mechanism of its force transfer mechanism, and provide theoretical basis for engineering practice.

2. Finite element analysis model establishment

2.1 Unit type and grid division

The FEM model producing the specimen is shown in Figure 1, which is modeled for 1/4 of the specimen given the structural symmetry[1]. Steel, through-steel and concrete slabs are defined and modeled using three-dimensional eight-node solid units , and reinforced bars are defined and modeled using three-dimensional two-node beam units . To improve the computational efficiency and accuracy, the FEM model adopts a different grid density for each component, where the grid size of the steel plate is 8mm^3, The mesh size of the concrete slab is 10mm^3, The grid size through the steel bar is 6mm^3[2].

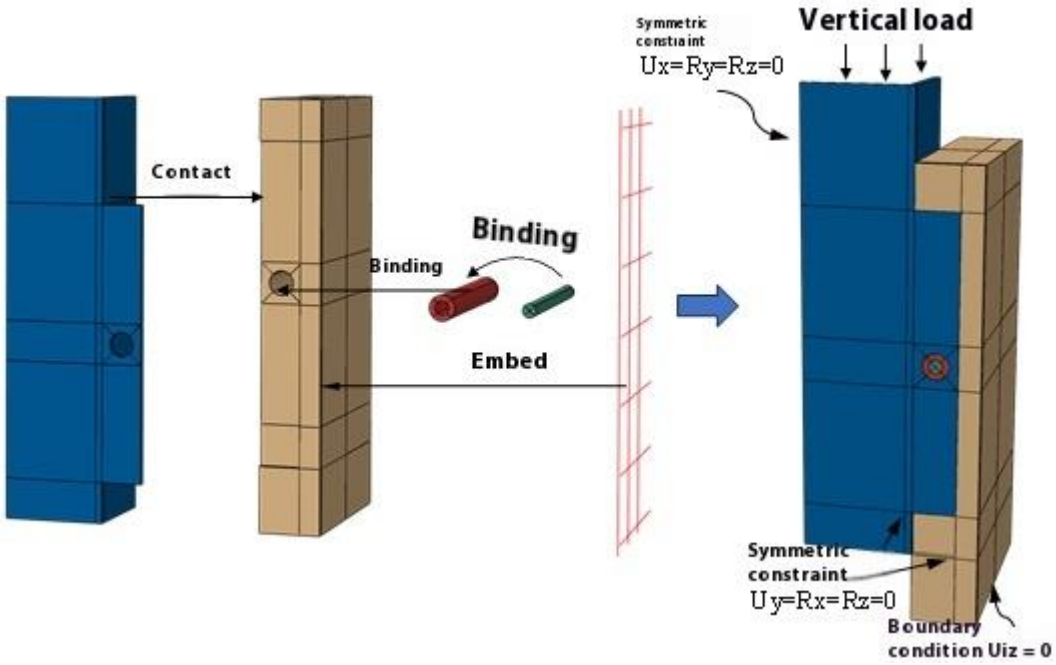

Figure 1: introduces the specimen finite element model

2.2 Border conditions and their interactions

Due to the symmetry of the structure, symmetry constraints are imposed on the surfaces of two symmetric planes (XOZ and XOY), and translational constraints along the x-and z-axis are applied to the x-plane and z-plane, respectively. The translation and rotational degrees of freedom in all directions on the surface of the concrete bottom plate are constrained. The interaction between the reinforcement and the surrounding concrete is defined using a "binding" constraint, and the reinforced reinforcement is "embedded" in the concrete slab. The interaction between the steel plate and the concrete contact surface is simulated using a "Surface to Surface", the normal phase behavior of the contact surface is defined by using a "hard contact", and the tangential behavior is defined by using a "penalty" algorithm with a friction coefficient of 0.3[3].

2.3 Material stress-strain relationship

(1) The UHPC stress-strain relationship

The UHPC in this study was defined using the concrete plastic damage model in the Abaqus material library[4]. As shown in Figure 1, the stress-strain relationship during the UHPC uniaxial

compression is determined according to Yang Jian[5]The proposed UHPC uniaxial compression constitutive model is determined, whose expression is shown in Equation(1).

$$\sigma_c = \begin{cases} f_c \dfrac{n\xi - \xi^2}{1+(n-2)\xi} & (0 < \varepsilon_c < \varepsilon_{c0}) \\ f_c \dfrac{\xi}{2(\xi-1)^2+\xi} & (\varepsilon_{c0} < \varepsilon_c < \varepsilon_{cu}) \end{cases} \tag{1}$$

In formula: ε_{c0}=3500με; $\xi=\varepsilon_c/\varepsilon_{c0}$; ε_{cu}=20,000με; n= E_c/ E_s; $E_s= f_{cu}/\varepsilon_{co}$;$\varepsilon_{c0}$Is the peak pressure strain; ε_{cu}Is the ultimate pressure strain; E_cIs the elastic modulus; E_sIs the cut-line modulus of the peak point; f_cIs the UHPC compressive strength.

The uniaxial tensile stress-strain relationship of the UHPC was used by Wang et al[6]In publicity[7]The improved constitutive relationship based on the UHPC uniaxial elongation model can reflect the strain hardening characteristics of UHPC, and its stress-strain relationship and expression are shown in Figure 1 and equation (2) respectively.

$$\sigma_t = \begin{cases} \dfrac{f_{te}}{\varepsilon_{te}}\varepsilon_t & (0 < \varepsilon_t < \varepsilon_{te}) \\ f_{te} + \dfrac{f_{tu}-f_{te}}{\varepsilon_{tu}-\varepsilon_{te}}(\varepsilon_t - \varepsilon_{te}) & (\varepsilon_{te} < \varepsilon_t < \varepsilon_{tu}) \\ f_{tu}\dfrac{1}{1+[(\varepsilon_t-\varepsilon_{tu})/(\varepsilon_{0.5}-\varepsilon_{tu})]^{1.3}} & (\varepsilon_{tu} < \varepsilon_t) \end{cases} \tag{2}$$

In formula: ε_{te}= 250με; ε_{tu}=3050με; ε_{te}Is the elastic limit tensile strain; ε_{tu}Is the ultimate tensile strain; $\varepsilon_{0.5}$Is 0.5 times the decrease in the segment of f_{tu}Corresponding strain.

Compressed injury factor d of UHPC$_c$And with the compression plastic strain ε_c, Available (3); pull damage factor d_tWith the tensile plastic strain of ε_tRelated, available equation (4).

$$d_c(\varepsilon_c^{in}) = \frac{(1-0.7)\varepsilon_c^{in}E_c}{\sigma_c + (1-0.7)\varepsilon_c^{in}E_c}$$
$$\varepsilon_c^{in} = \varepsilon_c - f_c / E_c \tag{3}$$

$$d_t(\varepsilon_t^{in}) = -0.114 + 0.872(1-e^{-\varepsilon_t^{in}/5\times10^{-4}}) + 0.185(1-e^{-\varepsilon_t^{in}/0.014})$$
$$\varepsilon_t^{in} = \varepsilon_t - f_t / E_c \tag{4}$$

(2) Steel stress-strain relationship

The ideal elastic-plastic double folding line model is used to define and model the steel plate and reinforcement in the introduced specimen. The yield strength, elastic modulus and Poisson ratio parameters required for the calibration of the steel in the double folding line model are obtained from the basic material properties of the steel. The stress-strain relationship is shown in Figure 2.

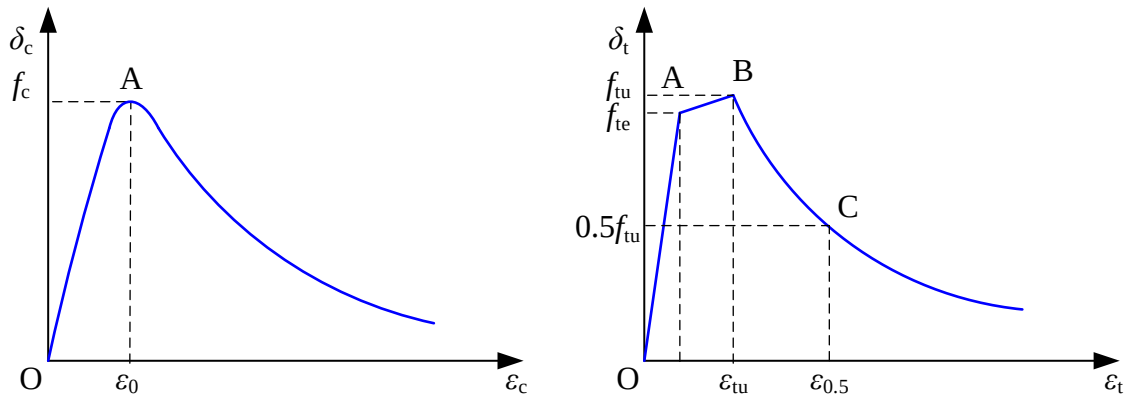

(a) Compressed constitutive model (b) The system is subject to the Laben structure model

Figure 2: The UHPC stress-strain curve

3. Finite-element model validation

Figure 3 shows the control results of the load-slip curve of the test and the load-slip curve of the finite element. It can be seen that the specimen has no different stiffness with the finite element model in the elastic stage, and the two curves highly coincide. As the load increases, the finite element curve gradually falls below the experimental curve in the elastoplastic stage, and both curves increase slowly after entering the plastic stage, but the finite element curve is gradually higher than the experimental curve. After reaching the peak load, the load-slip curve of the specimen falls spontaneously and enters the softening section, while the finite element curve lands slowly at the peak load. The peak load and limit slip of the finite element curve are slightly higher than the experimental curve. In general, the coincidence between the finite element curve and the experimental curve is high. The reason why the finite element curve is lower than the test curve in the elastic-plastic stage may be that the improvement effect of steel fiber on the shear resistance of PBL connector cannot be simulated in the numerical analysis. In addition, the peak load and limit slip of the finite element simulation are slightly higher than the test results, which may be because the numerical simulation cannot simulate the sudden fracture of the reinforcement through the test. Therefore, so when the test curve reaches the peak point, the finite element curve still increases slowly, and then the load gradually decreases.

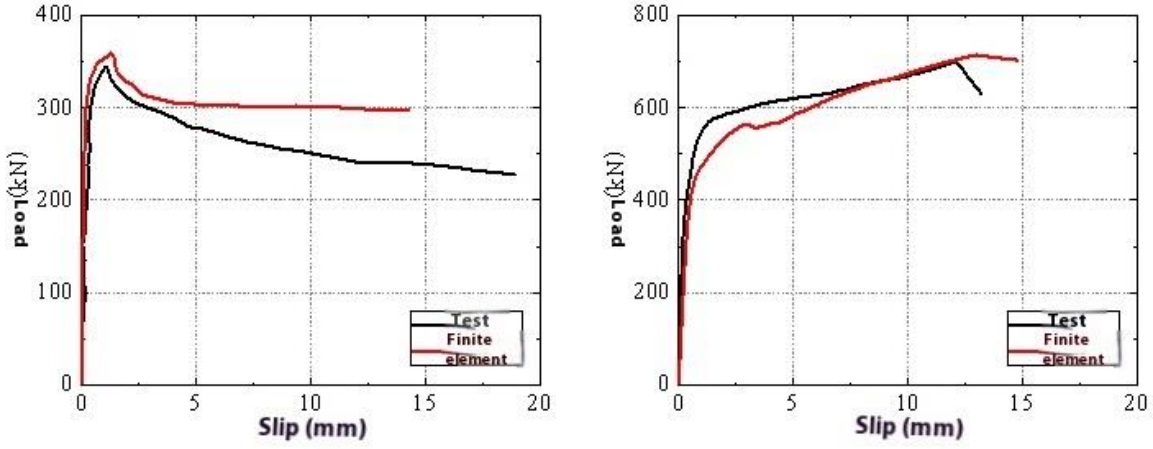

(a) PS-1 (b) PS-2

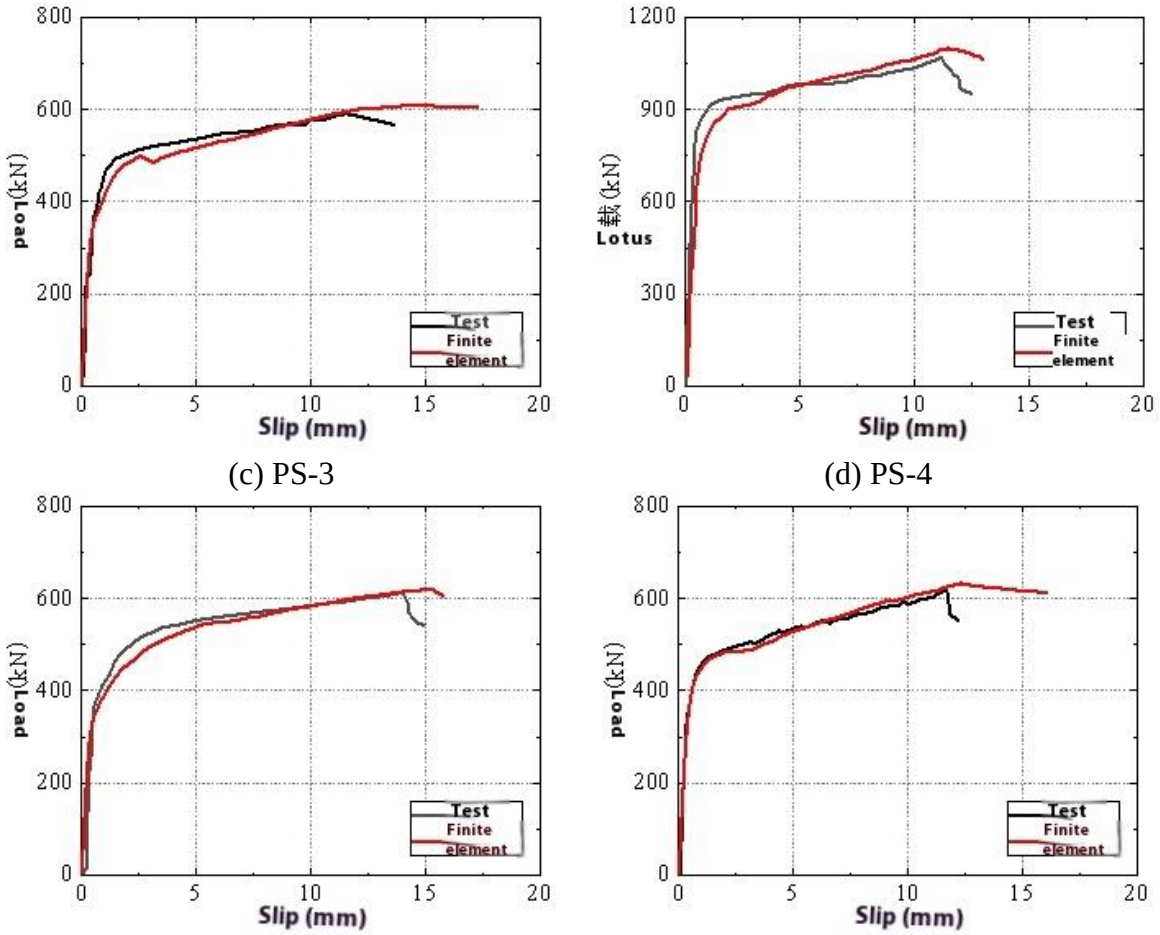

(c) PS-3 (d) PS-4

(e) PS-5 (f) PS-6

Figure 3 Load-slip curves with finite element

Table 1 shows the comparison results of the test between the peak load of the test and the finite element, and the ratio of the peak load between the test and the finite element and the ultimate slip ranges from 0.96~0.98 and 0.81~0.97. The finite element analysis results are slightly less than the test results, but the deviation is less than 10%, indicating that the finite element model established in this paper can accurately predict the carrying capacity of the specimen.

Table 1 Comparison of peak load and limit slip between test and FE

The specimen number	The test result		Finite element results		Pu,test/ Pu,fea	Su,test/ Su,fea
	Pu,test (kN)	Su,test(mm)	Pu,fea(kN)	Su,fea (mm)		
PS-1	344.55	1.04	358.93	1.29	0.96	0.81
PS-2	697.46	12.02	714.12	13 .01	0.98	0.92
PS-3	590.76	11.55	608.36	14.42	0.97	0.80
PS-4	1067.85	11.09	1098.19	11.46	0.97	0.97
PS-5	615.10	14.03	618.69	15.34	0.99	0.91
PS-6	620.10	11.63	632.78	12.36	0.98	0.94
mean					0.98	0.90

Figure 4 shows the comparison of the key elements in the FE simulation. It can be seen from Figure 4 that the failure of the specimen is mainly caused by the shear fracture of the steel bar. In the numerical simulation, great deformation is observed in the middle of the steel bar, which is

consistent with the test results. In addition, the hole wall of the open steel plate is deformed in the process of shear force transfer, and it is also observed in the numerical simulation. It can be seen that the finite element simulation can better reflect the stress state of the PBL connector. Therefore, the analysis of the load-slip curve and the force state of the specimen can accurately predict the whole force process of the connectors, and further reveal the destruction mechanism and force transfer mechanism.

(a) Open-hole steel plate (b) runs through the reinforcement

Figure 4 compares the failure results between the tests and the numerical simulations

4. Analysis of the force transmission mechanism of the PBL connector in UHPC

Experimental research can directly reflect the authenticity of a structure or system with high reliability, but it is often constrained by manpower, time, and cost. When supplementary test samples or expanded research scopes are required, the finite element simulation method offers a flexible alternative. This approach enables rapid model modification and analysis, thereby reducing the number of physical tests needed. Additionally, it can directly visualize micro-level stress distribution and deformation patterns. Based on the established finite element model, this study investigates the stress status of PBL connection components throughout their entire loading process, aiming to reveal the internal force transmission mechanism within PBL connections.

Figure 5~7 shows the cloud map of the stress distribution of the introduced specimen PS-3 in the elastic and elastic-plastic stages and plastic stages. From Figure 5, we can conclude that when the load is 0.3 times the peak load, the slip amount is 1mm, and the specimen is in the elastic stage. At this time, the interface between the steel beam and the concrete plate slips, and the shear force is transferred from the steel beam to the concrete tenon, and the upper wall of the open steel plate and the concrete tenon collide, which leads to the large stress on the top of the concrete tenon. Due to the downward decrease of shear transmission, the stress generated through the reinforcement is small, and gradually reduced from the middle to the two ends. In the elastic stage, the contact position of the open steel plate and the concrete tenon is the maximum stress, but not exceeding the yield strength. At this stage, the shear force is mainly the concrete tenon and penetrating steel bar, but the load proportion of concrete load is higher than that of the penetrating steel bar.

When the load reaches 0.6 times the peak load, the slip amount reaches 11mm. From Figure 6, we can see that the concrete tenon has reached the yield stress, and the through reinforcement below is about to yield, the specimen is in the elastic-plastic stage, and the slope of the corresponding load-slip curve is significantly reduced, and the inflection point appears. At this stage, the load ratio of the concrete tenon is higher than that of the penetrating steel bar, but with the increase of the load, the concrete tenon gradually enters the plastic state and damages, and the load ratio of the penetrating steel bar is increasing, and the yield of the penetrating steel bar at the load-sliding curve.

Figure 7 shows that when the load reaches 0.9 times of the peak load, the stress distribution of each component can show that the concrete tenon has been obviously damaged, and the penetrating steel bar has also yielded, but the limit strength has not been reached, so the load-slip curve still rises slowly and is about to reach the limit state. As the load reaches the ultimate strength of the through steel bar, the through steel bar is damaged, the through steel bar breaks in the

corresponding launch test, and the specimen loses the bearing capacity.

Figure 5 Stress distribution status of each component in the elastic phase

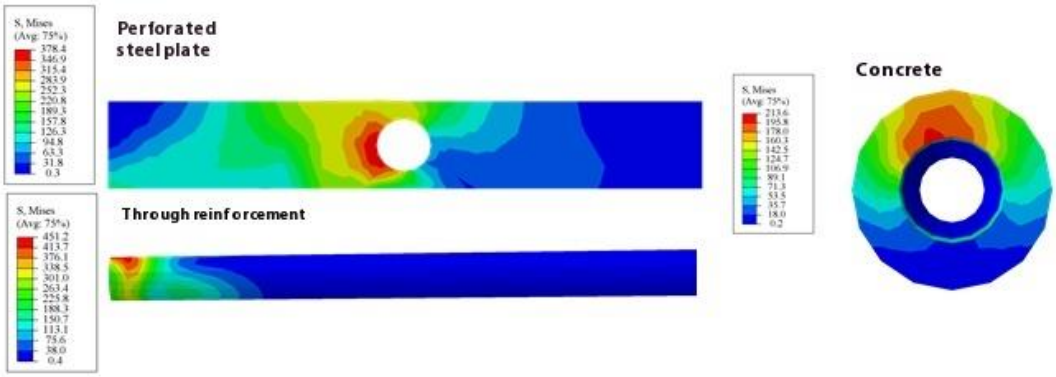

Figure 6 Stress distribution status of each component in the elastic-plastic phase

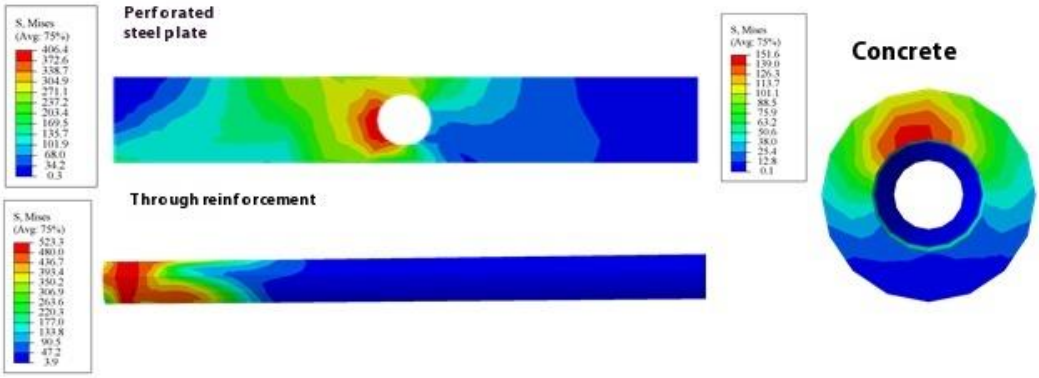

Figure 7 Stress distribution status of each component in the plastic phase

5. Parameter analysis

In order to comprehensively study the influence of different parameters on PBL connectors, based on the verified finite element model of specimen PS-3 in Section 3, the finite element model involving UHPC compression strength, opening plate thickness, through reinforcement yield strength and opening diameter variables was established for numerical analysis. The detailed parameters and results of the related model are shown in Table 2.

Table 2 Parameters and analysis results

The specimen number	T/mm	fy/ MPa	fc/ MPa	D/mm	Pu,fea
U100	14	4 50	100	50	632.78
U120			120		714.12
U140			140		773.1
U160			160		824.46
T10	10		120		615.1
T12	12				689.31
T14	14				697.46
T16	16				673.76
Y345	14	345			593.4
Y400		400			670.35
Y500		500			740.36
D40		450		40	540.36
D50				50	714.12
D60				60	873.68

(1) The UHPC compressive strength

With other parameters, a finite element model of UHPC compression strength 100MPa, 120MPa, 140MPa and 160MPa finite element model of specimen PS-3 was established to study the effect of different UHPC compressive strengths. Figure 8 shows a linear relationship of ultimate bearing capacity with UHPC compressive strength. When the UHPC compressive strength increased from 100MPa to 120MPa, the ultimate bearing capacity increased from 632.78kN to 714.12kN, by 13%, and when the UHPC compressive strength increased from 120MPa to 160MPa by 8.3% and 6.6%, respectively. Because the increase of UHPC strength drives the shear ability of the concrete tenon in the open steel plate, the concrete tenon and the penetrating steel bar bear the shear force together, so that the overall shear ability of PBL connector is improved. Therefore, it is concluded that improving the compressive strength of UHPC can improve the shear ability of PBL connector.

(2) Thickness of the open-hole steel plate

With other parameters, the FE model of 10mm, 12mm, 14mm and 16mm was based on the basis of specimen PS-3 to study the effect of different open plate thickness. Figure 8 can see that as the thickness of the open steel plate increases from 10mm to 16mm, the ultimate bearing capacity shows a trend of first increasing, then unchanged, and finally decreasing. When the thickness of the opening plate increased from 10mm to 12mm and 14mm, the ultimate bearing capacity increased by 12% and 1.2%, respectively, but when the thickness of the opening plate increased from 14mm to 16mm, the ultimate bearing capacity decreased by 3.3%. The reason is that when the thickness of the open steel plate is small, it will be damaged prematurely in the process of shear transmission, and the shear contribution of concrete tenon and penetrating steel bar cannot be played, resulting in the low bearing capacity of PBL connector. Increasing the thickness of the open steel plate can increase the contact area of the steel plate and the concrete tenon, and then improve the shear strength of the concrete tenon. When the thickness of the open steel plate increases from 12mm to 14mm, the shear capacity only increases by 1.2%, and when the thickness of the open steel plate exceeds 14mm, the shear capacity decreases, which indicates that when the thickness of the open steel plate is large, the deformation of the through steel bar is limited, leading to the decrease of the shear contribution of the through steel bar. Therefore, the choice of the best thickness of the open steel plate is conducive to play the material properties of each component, and should be considered. The ductility reduction caused by the thickness of the open-hole steel plate.

(3) The yield strength through the reinforcement

To study the effect of yield strength, finite element models of 345MPa, 400MPa and 500MPa 3 were established for analysis. As can be seen from Figure 8 , the increase in the yield strength through the reinforcement leads to a significant increase in the ultimate bearing capacity. When the yield strength of the through steel bar increased from 345MPa to 400MPa and 500MPa, the bearing capacity increased from 279 kN to 670.35kN and 740.36kN, increasing by 13% and 9.6%, respectively. The yield strength of through the reinforcement has a significant impact on the ultimate bearing capacity of the PBL connector, which is manifested by the linear growth of the ultimate bearing capacity with the increase of the yield strength of through the reinforcement.

(4) Opening diameter

Finite element models with opening diameters of 40mm, 50mm and 60mm were established to study the influence of opening diameter. As can be seen from Figure 8 , the ultimate bearing capacity increases linearly with the opening diameter. When the opening diameter increases from 40mm to 50mm and 60mm respectively, the bearing capacity increases from 540.36kN to 714.12kN and 873.68kN, increasing by 32.1% and 22.4%. Increasing the opening diameter can expand the contact area of the concrete tenon, thus strengthening the resistance of the concrete tenon. Therefore, the opening diameter has a significant impact on the performance of the PBL connector, and the increase of its diameter helps to improve the ultimate bearing capacity of the connector.

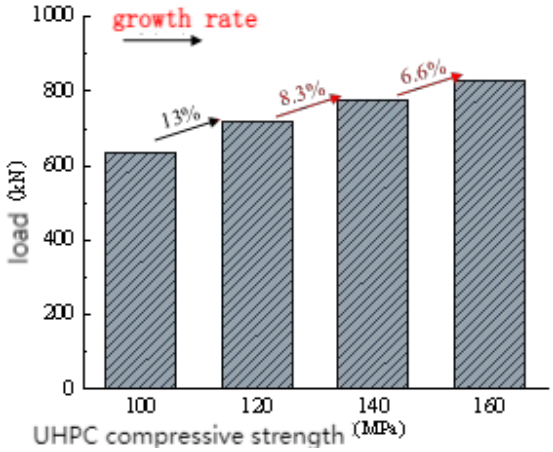

(A) The UHPC compressive strength

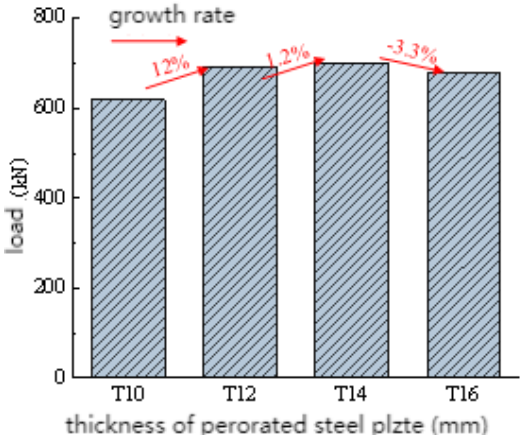

(B) Thickness of the opening steel plate

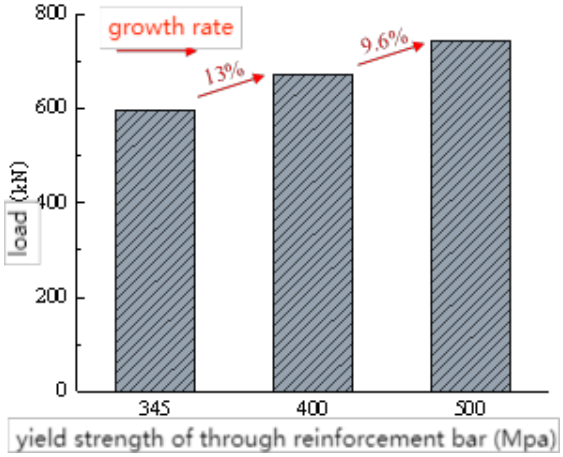

(C) the yield strength through the reinforcement

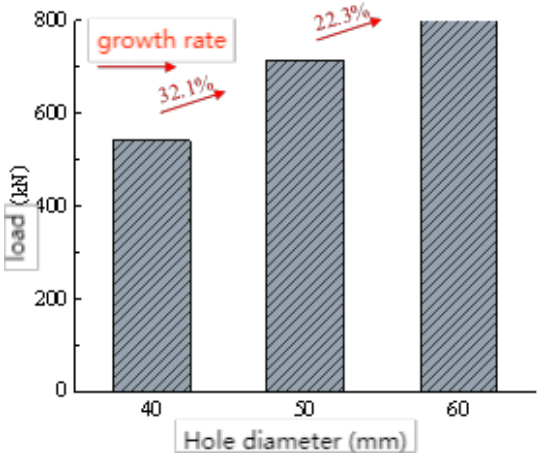

(D) Open hole diameter

Figures 8 The effects of the different parameters

As demonstrated in the above analysis, the shear resistance of the concrete tenon and reinforcement constitutes the primary factors affecting the shear capacity of PBL joints. These critical parameters include the concrete tenon's contact area, compressive strength, and the yield strength of the through reinforcement. While some secondary factors do not directly contribute to the joint's load-bearing capacity， they indirectly influence the connection by affecting the material performance of associated components. For instance, optimizing the thickness of the perforated steel plate ensures the full utilization of the concrete tenon and reinforcement's shear resistance. Such factors，though not dominant, remain essential considerations in the comprehensive evaluation of PBL joint behavior.

6. Conclusion

In this paper, ABAQUS software is used to further study the stress performance of the PBL connector. The results of the finite element model are consistent with the test load-slip curve and damage mode, indicating that the finite element model can accurately reflect the stress state of the PBL connector. Then, the whole process of the specimen was analyzed, and the force transmission mechanism of PBL connector was revealed by studying the stress distribution of each component. Finally, the effects of UHPC compressive strength, opening plate thickness, penetration reinforcement yield strength and opening diameter on the mechanical properties of PBL connections were analyzed by experimental parameters. The main conclusions are obtained as follows:

(1) The load-slip curve of the finite element model is basically consistent with the test curve, and the ratio of the peak load of the test and the finite element ranges from 0.96 to 0.98, with the error within 10%. In addition, the failure pattern of the reinforcement fracture in the test is consistent with the large deformation through the middle of the finite element analysis. It can be obtained that the finite element model can more accurately introduce the carrying capacity and stress state of the specimen.

(2) In the elastic stage, the maximum stress is the contact position of the open steel plate and the concrete tenon, but it has not yet exceeded the yield strength. In this stage, the shear force is mainly borne by the concrete tenon and the through steel bar, but the load proportion of the concrete is higher than that through the steel bar. In the elastic-plastic stage, the load ratio of concrete is higher than that of the penetrating steel bar. As the load increases, the concrete tenon gradually enters the plastic state and damages, and the load ratio of the penetrating steel bar is gradually higher than that of the concrete tenon. In the state of extreme damage, the concrete tenon has been obviously damaged, and the through reinforcement has also surrendered, but it has not yet reached the limit strength, until the specimen loses the bearing capacity after the through reinforcement reaches the limit strength.

(3) The compressive strength of UHPC has a significant impact on the mechanical properties of PBL connector, and increasing the compressive strength of UHPC can improve the shear bearing capacity of PBL connector. Increasing the thickness of the open steel plate can avoid its premature yield, ensure that the shear strength of the concrete tenon and through the steel bar is given full play, which is conducive to improving the shear capacity of the PBL connector. However, when the thickness of the open steel plate is large, it will also limit the deformation of the through steel bar, leading to the decrease of the shear contribution of the through the steel bar.

(4) The yield strength of the steel bar has a significant impact on the ultimate bearing capacity of the PBL connector, and the ultimate bearing capacity increases linearly with the yield strength of the steel bar. Increasing the opening diameter improves the contact area of the concrete tenon, which can significantly improve the ultimate bearing capacity of the connector.

References

[1] Hu Y, Meloni M, Cheng Z, et al. Flexural performance of steel-UHPC composite beams with shear pockets[C]//Structures. Elsevier, 2020, 27: 570-582.
[2] Yan J B, Li Z X, Xie J. Numerical and parametric studies on steel-elastic concrete composite structures[J]. Journal of Constructional Steel Research, 2017, 133: 84-96.
[3] Ding J, Zhu J, Shi T. Performance of grouped stud connectors in precast steel-UHPC composite bridges under combined shear and tension loads. Engineering Structures 2023:277:115470.
[4] Q.H. Han, Y.H. Wang, J. Xu, Y. Xing, Static behaviour of stud shear connectors in elastic concrete-steel composite beams, J. Constr. Steel Res. 113 (2015) 115–121.
[5] Yang Jian, Fang Zhi. Study on the compressive stress-strain relationship of ultra-high performance concrete [J]. Concrete, 2008, (07): 11-15.
[6] Wang J Y, Gao X L, Yan J B. Developments and mechanical behaviors of steel fiber reinforced ultra-lightweight cement composite with different densities[J]. Construction and Building Materials, 2018, 171: 643-653.
[7] Zhang Zhe, Shao Xudong, Li Wenguang, et al. Ultra-high performance concrete shaft tensile performance test [J]. Highway Journal of China, 2015,28 (08): 50-58.